nzsee
NEW ZEALAND SOCIETY FOR EARTHQUAKE ENGINEERING

Energy Considerations for Estimating Displacements of Oscillators with Different Hysteresis Shapes

M. Farshbaf & A. S. Moghadam
Department of Structural Engineering, International Institute of Earthquake Engineering and Seismology (IIEES), Iran.

G. A. MacRae & C-L. Lee

Department of Civil and Natural Resources Engineering, University of Canterbury, Christchurch, New Zealand.

H. Soleimankhani

Holmes Consulting, Christchurch, New Zealand.

T.L. Chang

Institut für Physik, Humboldt-Universität zu Berlin, Berlin, Germany.

ABSTRACT

This paper evaluates the number of cycles of deformation, N_c, of single degree of freedom (SDOF) structures with different hysteresis loop shapes subjected to earthquake loading because this influences both the peak displacement and the damage in a structure. The open-source software OpenSEES was modified to allow flag-shaped hysteresis loops ranging from elastic bilinear (with no energy dissipation) to traditional bilinear. To address the current inconsistency in the literature the concept of oscillation resistance ratio (ORR) has been introduced before. A relationship to estimate (ORR) for oscillators with different displacement ductility and a flag-shaped hysteresis loop is developed under free vibration, assuming no damping and no strain hardening. This relationship, initially developed using simple mechanics considerations, is then compared with that found from a time history analysis. The relationship is then extended to consider the effects of tangent stiffness proportional damping. The number of oscillation cycles, N_c, is defined as the number of post-initial elastic displacement excursions obtained during shaking to the number in one full cycle to the same peak displacement. Relationships between N_c and ORR were developed for structures with lateral force reduction factor, R, period, T, and damping assuming no strain hardening using a suite of 9 earthquakes records.

It was found that estimated ORR for the mechanics-based method and time history analysis considering free vibration were identical for all flag shape loop shapes. For a damping ratio of 5%, the ORR obtained increased by less than 12% compared to 0% damping for the flag-shaped parameters greater than 0.2. As a result, the

ORR for a loop with no damping was used in the remainder of the paper. In general, as the ORR decreased to less than 0.3 (i.e. the hysteresis loop had less energy dissipation), N_c increased. It was found that N_c was insensitive to the lateral force reduction factor, but increased for lower damping when ORR was less than 0.3. Also, it increased for shorter period oscillators when ORR was less than 0.3, but the trends were less clear with greater *ORR*.

1 INTRODUCTION

Since seismic damage is directly correlated to the displacement (deformation) of the structure, the estimation of displacements plays a significant role in seismic response estimation. There are many ways of predicting displacement. Two simple empirical approaches are commonly used in design as the basis for the prediction of structural displacement demand by engineers. The first one, which is the basis of many common design standards, computes displacements of the structures based on their initial stiffness and does not consider the hysteretic damping effect. This method is independent of the structure's unloading and energy dissipation characteristics. A second approach is based on the structure's secant stiffness and hysteresis damping. This approach is more often used for structures with pinched hysteretic behaviour. Nevertheless, differences in response estimation exist for these two methods as a result of the fundamental assumptions, the type of earthquake record used, and the specific calibration performed.

A new method to possibly reconcile these two approaches uses Oscillation Resistance Ratio (ORR) for estimation of maximum displacement and indicates that ground motion duration is important but so far limited studies have been conducted in this area (Soleimankhani et al., 2021).

In order to predict displacements for a range of hysteresis loops, and reconcile the difference between different approaches, there is a need to understand the parameters, and the relationships between them.

This paper seeks to address this need by seeking answers to the following questions:

1. What key parameters affect the peak seismic displacements of structures with different hysteresis loops?

2. Can the key hysteresis loop parameters be related with adequate accuracy to the peak displacement?

3. How do the lateral force reduction factor (R), period (T), damping, and ground motion characteristics affect the parameters selected?

1.1 Literature review

1.1.1 Initial and secant stiffness-based displacement prediction methods

Initial stiffness-based methods use the assumption that inelastic response may be predicted from elastic response. Two widely known relationships, based on initial stiffness are the equal displacement assumption (EDA) and equal energy assumption (EEA) (Veletsos and Newmark, 1960), which are the basis of common standards such as FEMA 356 (ASCE 2000), EDA principle often assumes in design that for medium to long period structures, the inelastic displacement is equal to the displacement of an equivalent elastic system with the same initial stiffness. EEA principle states for shorter period structures, the inelastic displacements are often larger than elastic displacements. FEMA 356 (ASCE 2000), based on Berrill et al. (1980), introduces an empirical factor (C_1) to modify the displacement calculated for the linear response to the inelastic response for short period structures. The displacement demand of an inelastic system may be affected by the hysteretic characteristics of the structural elements. According to FEMA 356, for structures with low energy dissipation such as pinched hysteretic structures (e.g. rocking structures), EDA may underpredict the actual displacements so modifications have been proposed for a more accurate displacement demands estimation (i.e. the C_2 factor) to represent the effect of pinched hysteresis shape.

The idea of using an elastic substitute structure was first introduced by Jacobsen (Blandon and Priestley, 2005). His approach, followed by Gulkan (Sozen, 2017), is based on the concept that the energy absorbed by the hysteretic cyclic response of a yielding structure in its steady state is equal to the energy dissipated by the equivalent viscous damping (EVD) of a substitute structure, ξ_{hyst}, with an elastic stiffness equal to the secant stiffness at the peak displacement. This is expressed in Equation (1). This approach is adopted in documents such as ATC-40. It provides procedures for the seismic evaluation and retrofit of concrete buildings (ATC1996). Modifications are also made to this approach to better fit the results of actual oscillators.

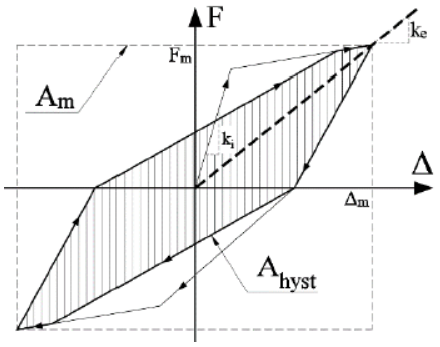

Figure 1: Hysteresis Area for EVD calculation

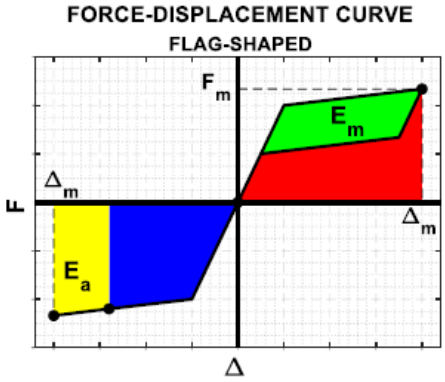

Figure 2: Definition of E_a (Flag-shaped hysteresis) (Soleimankhani et al., 2021)

$$\xi_{eq} = \xi_0 + \xi_{hyst} = \xi_0 + \frac{2}{\pi}\frac{A_{hyst}}{A_m} = \xi_0 + \frac{A_{hyst}}{2\pi F_m \Delta_m} \quad (1)$$

where ξ_0 = initial elastic damping ratio;

A_{hyst} = complete stabilized hysteresis loop area, the hatched area shown in Figure 1;

A_m = rectangular area within the maximum force, F_m, and displacement, Δ_m as shown in Figure1.

1.1.2 Oscillation Resistance Ratio (ORR)

The ORR concept, illustrated in Figure 2 and Equation 2, may unify the initial stiffness method with the secant stiffness method (Soleimankhani et al., 2021). For an oscillator which has reached its peak displacement in one direction, the ORR is defined as the energy required to be input into the system so that it has a greater displacement in the opposite direction than in the initial direction (shown as the yellow area E_a in Figure 2), divided by two times the strength at peak displacement, F_m, multiplied by the peak displacement of the structure, Δ_m. The term $2F_m\Delta_m$ is simply a convenient normalization resulting in ORR ranging between zero and unity for loops without degradation and no post-elastic stiffness.

$$ORR = \frac{E_a}{2F_m\Delta_m} \quad (2)$$

The green plus red area in Figure 2, is the monotonic loading energy required to reach the peak displacement assuming no viscous damping. The hysteretic energy dissipated during the first half cycle is shown by the green area. The area above the horizontal axis and below the unloading path of the hysteretic response shown by the red area is the potential energy, or the recoverable strain energy stored in the system. When the system is released from its peak displacement and permitted to oscillate in free vibration, then the potential energy of the structure is converted into kinetic energy at zero force. The momentum at this point then causes the structure to move towards its peak displacement in the opposite direction as shown by blue areas (MacRae et

al., 2020), where the blue area is the same as the red area. For very short duration records, such as impulsive ones, the oscillator response is almost monotonic, and the peak displacement is independent of the unloading characteristics of the loop. Also, for oscillators with high ORR, it would be expected that significant oscillation would not occur, as it is difficult to obtain larger displacements in the opposite direction. However, for oscillators affected by long duration shaking, increased displacements due to oscillation are possible, and this may explain why short period structures are often considered to have higher displacement increases than long period ones. It seems that in addition to ORR, the number of cycles of shaking that the structure of a certain period is subject to is a key parameter affecting the displacements. This has been demonstrated to be the case by Soleimankhani et al. (2021), so it is desirable to quantify this effect.

2 METHODOLOGY

A single-storey numerical model with eleven different hysteresis shapes is employed in this study using OpenSEES (McKenna, Fenves and Scott, 2000). The system dissipates input seismic energy using the hysteresis loop described in Figure 3. Here, as the parameter β changes from zero to unity with no strain hardening (i.e. r = 0), the loop changes from bilinear elastic to elastic perfectly plastic as shown in Figure 4. For different target fundamental periods, T, assuming a specified mass, M, the system initial stiffness, K_i, was calculated using Equation (3). Also, the system lateral yield strength, F_y, was given by Equation (4) where g is the acceleration of gravity and S_a is the spectral acceleration.

$$K_i = \left(\frac{2\pi}{T}\right)^2 M \tag{3}$$

$$F_y = \frac{S_a . M . g}{R} \tag{4}$$

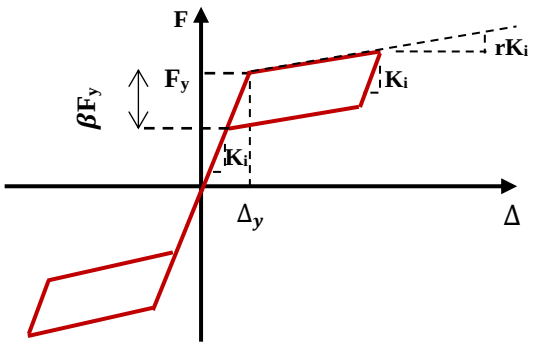

Figure 3: Flag-shape hysteresis curve

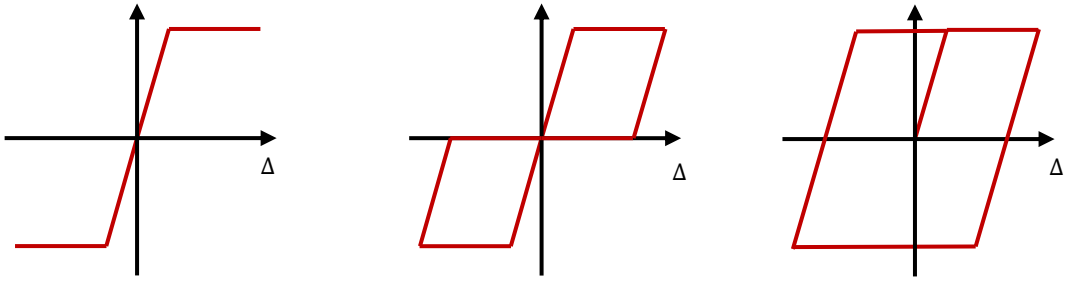

(a) β = 0, *bilinear elastic* *(b)* β = 0.5 *(full flag)* *(c)* β = 1.0 *(elastoplastic)*

Figure 4: Flag-shaped material (r = 0)

2.1 ORR calculation

Two methods are considered to calculate ORR, based on the assumption of free vibration. The first is by hand and can be used if there is no viscous damping. The second uses time history analysis (THA) with a computer. Figure 5 shows that if a structure reaches the displacement at the upper right part of the hysteresis loop, and then oscillates in free vibration (ignoring damping) then it will release potential energy and use that energy again as it moves in the opposite direction, so the shaded areas are equal. It moves to the displacement associated with free vibration, Δ_{fv}, which is less than the peak displacement, Δ_p. For the oscillator to oscillate further in the reverse direction, it needs to have the energy E_a input into the system. Here, it may be seen that the bilinear loop requires substantially more energy (i.e. E_a) to cause oscillation in the reverse direction than does the flag-shaped loop. Therefore, oscillation is less likely, and the likelihood of increased displacements is reduced. The required additional input energy, E_a, can be calculated considering the shaded areas and the loop shape. This was done directly using the hand method and the ORR calculated according to Equation (2). In the THA method, the structure was first pushed to the maximum displacement and then released to vibrate freely to find Δ_{fv}. Again E_a, and the ORR were calculated in the same way as in the hand method.

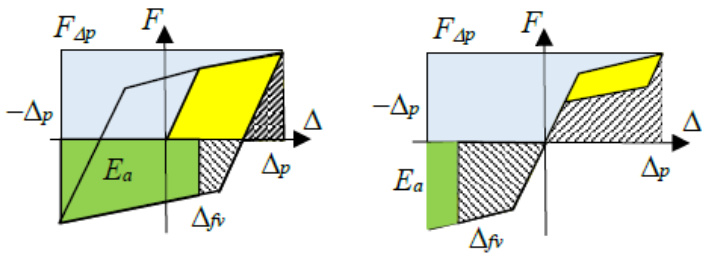

(a) High E_a and ORR *(b) Low E_a and ORR*

Figure 5: E_a for Different Hysteresis Loops (MacRae et al. 2020)

2.2 Number of Cycles of Deformation, N_c

To estimate the effective duration of the earthquake shaking, a number of methods have been proposed. For example, Trifunac and Brady (1975) compute this duration from a plot of the cumulative ground acceleration squared as a function of time. For structure-specific measures, the shaking experienced may be computed as an effective number of cycles of shaking considering the total hysteretic energy dissipated divided by that during one cycle (e.g., MacRae and Kawashima, 1993), or by a cumulative inelastic ductility (e.g., MacRae et al., 1990, Hancock and Bommer, 2005).

In this paper, a cumulative displacement method based on MacRae et al. (1990, 2009) is used to compute the effective number of cycles of shaking experienced, N_c, according to Equation (5) where the cumulative inelastic deformation (*CID*) is obtained by summing of inelastic deformation of the structure during the shaking, as shown in Figure 6. Similarly, the single-cycle cumulative inelastic deformation (*CIDS*) is obtained from the maximum and yielding deformations as shown in Figure 7. It is independent of β as shown in Equation (6).

$$N_c = \frac{CID\ (\beta,\ R, \zeta, T\ ;\ r = 0)}{CIDS\ (\beta,\ R, \zeta, T\ ;\ r = 0)} \tag{5}$$

$$CIDS = (\Delta_{max} - \Delta_y) \times 4 \tag{6}$$

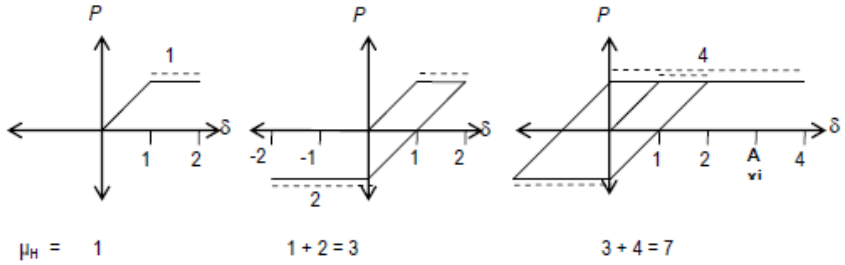

Figure 6: EPP model showing cumulative inelastic ductility (MacRae et al., 2009)

(a) Low ORR loop, β≅0.25 *(b) Higher ORR loop, β=0.5*

Figure 7: Single Cycle Cumulative Inelastic Deformation (CIDS) Calculation

A number of methods to compute a measure of the number of cycles of shaking have been trialled (Farshbhaf, 2024). One considering the hysteretic energy dissipated in the shaking divided by that in one cycle was not used because, in the case of $\beta = 0$ the ratio tends to infinity because the energy in one cycle is zero. Even the definition in Equation (5) is problematic when $\beta = 0$ and $\zeta = 0$ because oscillation continues forever so results for this case are not considered.

The model is subjected to 9 earthquake far-field records from FEMA P695 Appendix A listed in Table 1. OpenSees (McKenna et al., 2000) is used to perform the THA using the Newmark integration scheme with a time step, Δ_t, of 0.005s. The equivalent viscous damping for the translational mode of vibration is assigned and tangent stiffness proportional model is used. The mass proportional damping coefficient is ignored to provide a more realistic estimation of the system damping (Calvi et al., 2007).

Table 1: Far-field Records Used for THA (FEMA P695 Appendix A)

ID	Event	Year	Station	Fault type	M_w[a]	T_g (s) Comp.1-2	Distance (km)		$V_{s(30)}$(m/s^2)
							Clst.[b]	Epi.[c]	
1	Northridge	1994	Beverly Hills Mulhol	Blind thrust	6.7	0.91-0.55	17.2	13.3	356
2	Northridge	1994	Canyon W Lost Cany	Blind thrust	6.7	0.59-0.71	12.4	26.5	309
3	Duzce, Turkey	1999	Bolu	Strike-slip	7.1	0.56-0.99	12.0	41.3	326
4	Imperial Valley	1979	Delta	Strike-slip	6.5	3.28-1.66	22.0	33.7	275
5	Imperial Valley	1979	El Centro Array #11	Strike-slip	6.5	1.76-0.74	12.5	29.4	196
6	Kobe, Japan	1995	Nishi-Akashi	Strike-slip	6.9	0.47-0.72	7.1	8.7	609

7	Kobe, Japan	1995	Shin-Osaka	Strike-slip	6.9	0.67-1.23	19.2	46	256
8	Kocaeli, Turkey	1999	Duzce	Strike-slip	7.5	3.86-0.51	15.4	98.2	276
9	Kocaeli, Turkey	1999	Arcelik	Strike-slip	7.5	1.24-9.28	13.5	53.7	523

[a] Moment magnitude.
[b] Closest distance from the recording site to the ruptured area (if available).
[c] Distance from the recording site to the epicentre.

3 SENSITIVITY STUDY

In Section 3.1 the ORR value is calculated using two methods (hand and numerical analysis). Then the effect of ductility and damping on ORR is investigated. Sections 3.2 to 3.4 examine the impact of the number of cycles of deformation, THA has been applied using the records introduced in Table 1 and the median of responses is considered as a representative of the behaviour.

3.1 Comparison of ORR using two methods

Computed ORR values are compared using the (i) hand and (ii) THA methods for models with no damping and from $\beta = 0$ (bilinear) to $\beta = 1$ (elastic perfectly plastic) in Figure (8). As expected, the ORR obtained using these two methods gave the same response. A greater ORR means there is less potential for oscillation and the response may be governed by one major inelastic yield excursion. As shown in Figure (8), for the bilinear elastically responding structure ($\beta = 0$) the ORR is zero so there is a greater likelihood of oscillation in the reverse (negative) direction. For an EPP structure ($\beta = 1$), the ORR is high and it is unlikely that there will be a greater displacement in the reverse direction under short duration earthquake records. However, if there is significant energy input, then the displacement in the reverse direction may still increase if there are many cycles of loading on, and lots of energy input into, the structure. As was seen in Figure 8, the ORR increases with increasing ductility. However, as the demand approaches the value associated with a ductility of about 4, the ORR curves in Figure 8 start to reduce slope and become flat, so for greater ductility, the ORR does not change much.

Since calculation of ORR in models with damping is difficult using hand analysis, the THA method has been used to investigate the effect of 5% viscous damping. As shown in Figure 9, where the oscillator is pushed to a ductility of 4 before being released in free vibration, the presence of damping in the models with small β (lower energy dissipation capacity) increases the ORR, thereby reducing the probability of oscillation in the reverse (negative) direction. As β increases, the effect of viscous damping on the ORR decreases. It can be concluded that increasing hysteretic damping has a greater effect on reducing the probability of oscillation in the reverse (negative) direction than the viscous damping, and the presence of viscous damping increases the ORR value less than 12% in models with β greater than 0.2. Greater increases in ORR may be expected if initial stiffness proportional damping had been used.

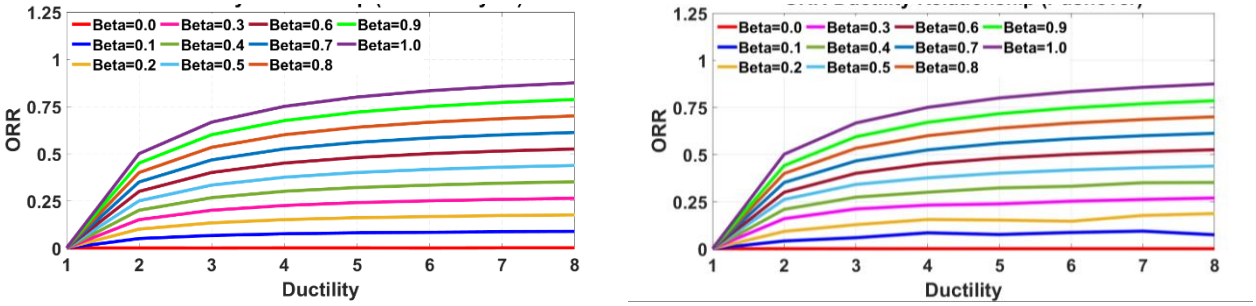

(a) Hand method *(b) THA method*

Figure 8: Effect of Ductility on ORR (μ = 4, ζ = 0)

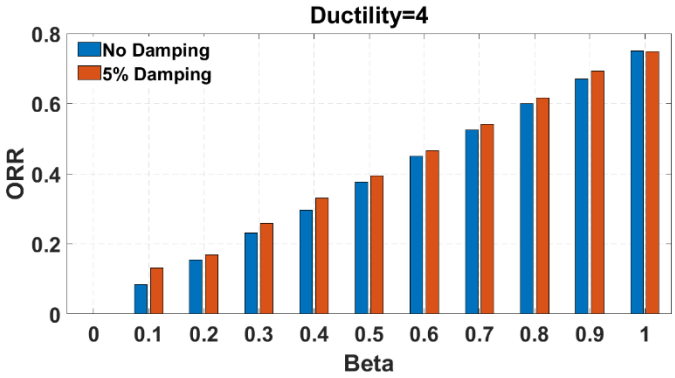

Figure 9: Effect of damping on ORR (μ=4, THA method)

3.2 Effect of *T* on N_c

THA with the suite of 9 records is performed to illustrate the effect of period, *T*, and ORR, on the number of cycles of deformation experienced due to the shaking, N_c. The records were scaled so that the lateral force reduction factor, *R*, for each record was 4. For ORR estimation, it was assumed for simplicity that the ductility, μ = *R*. Figure 10 shows that N_c that except for T=2s, the general trend was for greater N_c with lower ORR. Also, for the shortest period of T = 0.5s, N_c was generally greater than for longer periods. This is consistent with approaches used in many standards where for structures with a period less than about 0.7s, the peak displacements of an inelastically responding structure are generally greater than that of the elastic displacement. This is presumably because short period structures are subject to more cycles than longer period structures in a record of a specific duration. It is expected that N_c may be greater again for shorter period structures (e.g. 0.2 s).

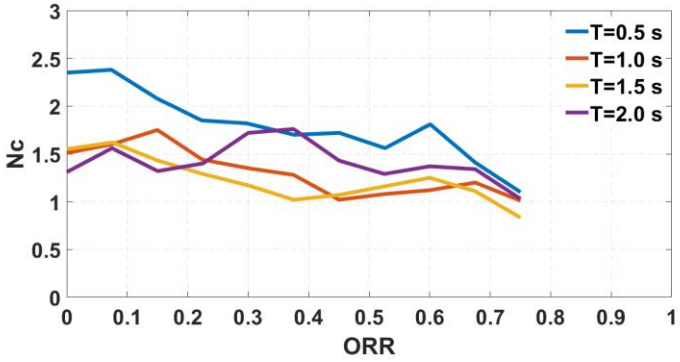

Figure 10: N_c versus ORR for different T
(Using R = 4 and assuming μ = R for ORR estimation, ζ = 5%, Record suite)

3.3 Effect of ζ on N_c

The effect of viscous damping, ζ, on the number of cycles of deformation, N_c, in a model with a period, T, equal to 1.0 second and a lateral force reduction factor, R, of 4 was investigated. Figure 11 shows that ζ did not have a significant effect on N_c particularly in models with high ORR. For ORR < 0.3, lower ORR was generally associated with a greater N_c. In these cases, increasing the damping has reduced N_c. For the model with no damping and ORR=0 ($\beta = 0$), there is nothing to stop the oscillation, so N_c may be infinite. This cannot be plotted so it is simply shown with the star.

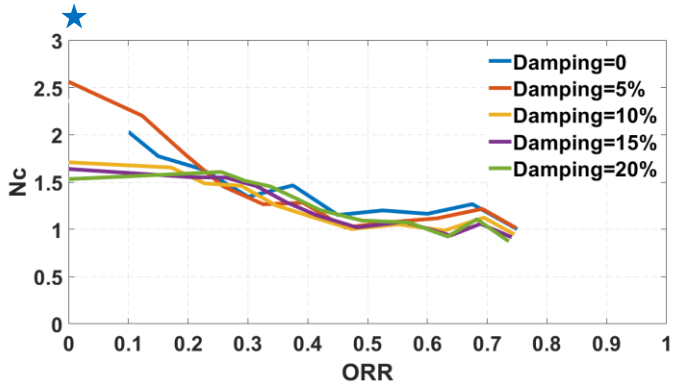

Figure 11: N_c versus ORR for different ζ
(Using R = 4 and assuming μ = R for ORR estimation, T=1.0 s, Record suite)

3.4 Effect of R on N_c

In order to investigate the effect of lateral force reduction factor on the number of cycles of deformation, models with different R, a period equal to 1 second (T=1.0 s), and 5% damping was studied. Figure 12 indicates higher R did not tend to reduce N_c. It is also noted that increasing R does not have a significant effect on ORR values.

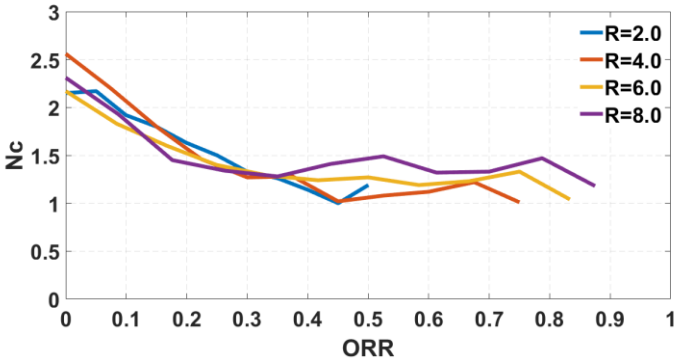

Figure 12: N_c versus ORR value for different R
(Assuming μ = R for ORR estimation, T=1.0 s, ζ = 5%, Record suite)

4 CONCLUSIONS

A study to understand the parameters affecting peak displacement of simple structures as a result of earthquake shaking. It was shown that:

1) Based on previous literature, it was hypothesized that key parameters were likely: i) hysteresis loop shape, represented by an oscillation ratio, ORR; ii) the level of inelasticity, represented by the lateral force reduction factor, R; and iii) the number of cycles of shaking, N_c, that the structure experiences.

To investigate this hypothesis, the OpenSEES software was modified to allow the effects of a range of hysteresis loops, ranging from elastic bilinear to elastic-perfectly plastic, to be characterised with one parameter β.

2) Two methods were developed to evaluate the relationship between the ductility μ and β to estimate the ORR. These methods were consistent and showed that for high β the ORR tended to converge. A method for describing N_c was also developed.

3) When N_c was plotted against ORR it was often relatively constant for ORR > 0.3 for the range of parameters investigated. For lower ORR, N_c increased. Variation of N_c with structural damping, ζ, and lateral force reduction factor, R, was relatively small for ORR > 0.3. N_c was greater for oscillators of shorter structural period, T, for all ORR. These findings are important for as part of the ongoing study to predict structural displacements.

5 REFERENCES

Berrill JB, Priestley, MJN, & Chapman, H E (1980). "Section 2 - Design earthquake loading and ductility demand". Bulletin of the New Zealand Society for Earthquake Engineering, 13(3), 232-241. https://doi.org/10.5459/bnzsee.13.3.232-241

Blandon, C. A., & Priestley, M. J. N. (2005). Equivalent viscous damping equations for direct displacement based design. Journal of earthquake Engineering, 9(sup2), 257-278.

Calvi, G. M., Priestley, M. J. N., & Kowalsky, M. J. (2007). Displacement-based seismic design of structures. New Zealand Conference on Earthquake Engineering.

Federal Emergency Management Agency (2000), "FEMA 356: Prestandard and Commentary for the Seismic Rehabilitation of Buildings". prepared by ASCE for the Federal Emergency Management Agency, Washington, D.C., 518 pp.

Farshbaf, M (2024), "Effect of hysteresis characteristics on maximum seismic displacements of self-centering reparable buildings". PhD Dissertation, International Institute of Earthquake Engineering and Seismology (IIEES), Iran.

Gulkan P and Sozen M (1974), "Inelastic Responses of Reinforced Concrete Structures to Earthquake Motions". ACI Journal, 71(12): 604-610.

Hancock, J., & Bommer, J. J. (2005). The effective number of cycles of earthquake ground motion. Earthquake engineering & structural dynamics, 34(6), 637-664.

MacRae G. A., Carr A. J. and Walpole W. R. (1990), "The Seismic Response of Steel Frames", Research Report 90-6, Department of Civil Engineering, University of Canterbury, New Zealand. Commissioned by the NZ Heavy Engineering Research Association.

MacRae G. A. and Kawashima K. (2000), "The Seismic Response of Bilinear Oscillators Using Japanese Earthquake Records", Journal of Research of the Public Works Research Institute, Vol. 30, Ministry of Construction, Japan.

MacRae, G. A., Urmson, C. R., Walpole, W. R., Moss, P., Hyde, K., & Clifton, C. (2009). Axial shortening of steel columns in buildings subjected to earthquakes. Bulletin of the New Zealand Society for Earthquake Engineering, 42(4), 275–287. https://doi.org/10.5459/bnzsee.42.4.275-287

MacRae, G. A., Zhao, X., Jia, L. J., Clifton, G. C., & Dhakal, R. (2020). The China-NZ ROBUST Friction Building Shaking Table Testing Overview.

McKenna, F., Fenves, G. L., & Scott, M. H. (2000), Open system for earthquake engineering simulation. University of California, Berkeley, CA.

Soleimankhani, H., MacRae, G., & Sullivan, T. (2021). The oscillation resistance ratio (ORR) for understanding inelastic response. Bulletin of the New Zealand Society for Earthquake Engineering, 54(4), 299–312. https://doi.org/10.5459/bnzsee.54.4.299-312

Standards New Zealand (2016), NZS1170.5: Structural Design Actions - Part 5: Earthquake actions - New Zealand Incorporating Amendment No. 1". Standards New Zealand, Wellington, New Zealand.

Trifunac, M. D., & Brady, A. G. (1975). A study on the duration of strong earthquake ground motion. Bulletin of the Seismological Society of America, 65(3), 581-626.

Veletsos S and Newmark N (1960), "Effect of Inelastic Behavior on the Response of Simple Systems to Earthquake Motions". Proceedings of Second World Conference on Earthquake Engineering, Tokyo, Japan.